

Article

# Run-Of-River Small Hydropower Plants as Hydro-Resilience Assets against Climate Change

Charalampos Skoulikaris 

Department of Civil Engineering, UNESCO Chair INWEB, Aristotle University of Thessaloniki, 54124 Thessaloniki, Greece; hskoulik@civil.auth.gr; Tel.: +30-2310995666

**Abstract:** Renewable energy sources, due to their direct (e.g., wind turbines) or indirect (e.g., hydropower, with precipitation being the generator of runoff) dependence on climatic variables, are foreseen to be affected by climate change. In this research, two run-of-river small hydropower plants (SHPPs) located at different water districts in Greece are being calibrated and validated, in order to be simulated in terms of future power production under climate change conditions. In doing so, future river discharges derived by the forcing of a hydrology model, by three Regional Climate Models under two Representative Concentration Pathways, are used as inputs for the simulation of the SHPPs. The research concludes, by comparing the outputs of short-term (2031–2060) and long-term (2071–2100) future periods to a reference period (1971–2000), that in the case of a significant projected decrease in river discharges (~25–30%), a relevant important decrease in the simulated future power generation is foreseen (~20–25%). On the other hand, in the decline projections of smaller discharges (up to ~15%) the generated energy depends on the intermonthly variations of the river runoff, establishing that runoff decreases in the wet months of the year have much lower impact on the produced energy than those occurring in the dry months. The latter is attributed to the non-existence of reservoirs that control the operation of run-of-river SHPPs; nevertheless, these types of hydropower plants can partially remediate the energy losses, since they are taking advantage of low flows for hydropower production. Hence, run-of-river SHPPs are designated as important hydro-resilience assets against the projected surface water availability decrease due to climate change.

**Keywords:** small hydropower plants; HEC-ResSim; run-of-river dams; climate change; hydrologic simulations; hydroelectric energy; Kalamas River; Axios River



**Citation:** Skoulikaris, C. Run-Of-River Small Hydropower Plants as Hydro-Resilience Assets against Climate Change. *Sustainability* **2021**, *13*, 14001. <https://doi.org/10.3390/su132414001>

Academic Editor: Dalia Štreimikienė

Received: 20 November 2021

Accepted: 15 December 2021

Published: 18 December 2021

**Publisher's Note:** MDPI stays neutral with regard to jurisdictional claims in published maps and institutional affiliations.



**Copyright:** © 2021 by the author. Licensee MDPI, Basel, Switzerland. This article is an open access article distributed under the terms and conditions of the Creative Commons Attribution (CC BY) license (<https://creativecommons.org/licenses/by/4.0/>).

## 1. Introduction

Hydropower is the most mature renewable energy source (RES), as it was operationally commissioned at the beginning of the 20th century [1]; it thus has the biggest penetration percentages in the energetic grid in comparison to other renewable energy sources. In the year 2020, and on a global scale, hydropower represented the highest share among all renewables in electricity generation; i.e., it accounted for 57.72% among renewable energy sources (4.034 TWh out of 6989 TWh of all RES) [2] and for more than 16.0% of the world's net electricity production [3]. The 4.034 TWh/y of hydroelectricity come from an installed capacity of 1120 GW, demonstrating an increase of 13.6% in comparison to the 3551 TWh/y generated in the year 2009 [1]. On the European Union (EU) scale and according to data from 2019 [4], about one third, i.e., 30.2%, of the 2778 TWh of generated electricity came from RES, in comparison to 18.3% of the year 2009, with the highest shares of 13.0%, 12.2%, and 4.5% (out of 30.2%) to be attributed to wind, hydropower, and solar sources, respectively. The current energy generation bloom from renewables in EU is mainly connected to solar and wind technologies, since solar power grew from 0.5% in 2009 to 4.5% in 2019, and wind turbines power increased from 4.5% in 2009 to 13% in 2019 [4], while at the same time the hydroelectricity generation is stabilized around 650 TWh with a total installed capacity of 230 GW [5].

The dependence of RES, including hydropower, on climatic variables, which are going to be radically altered spatiotemporally due to global climate change [6,7] impose new externalities on RES projects' viability. The latest outputs of the Intergovernmental's Panel on Climate Change (IPCC) Sixth Assessment Report (AR6) [8] set the Mediterranean basin as a hot spot in terms of climate change impacts, as did the previous assessment report (AR5) [9]. Specifically, there is high confidence that the projected summer temperature increase will be larger than in the global mean, resulting in an increase in agricultural and ecological droughts (medium confidence), as well as that the precipitation decline will enforce the trends towards augmented hydrological droughts (high confidence). AR6 also depicts that reduced summer precipitation in southern Europe is projected, starting from a 2 °C global warming level (high confidence). The foreseen alterations in the climate system will induce changes in the hydrological cycle, i.e., changes in temperature and precipitation patterns will modify the annual water budget as well as the timing and seasonality of river flows, affecting, amongst other impacts, the operation of hydropower plants (HPPs). For new HPPs, changes in water availability could either lead to the malfunction of the infrastructure or result in lost opportunity cost, by not taking advantage of higher water volumes [10]. Cherry et al. [11] conclude that the increasing number of studies on hydrologic impacts due to climate change have now established a solid scientific base that should be integrated into hydropower scoping, design, and management.

The derived uncertainties of climate change on HPPs, especially on large ones that have an immense capital investment cost, together with the undoubtable environmental and social impacts of conventional hydroelectric dams at basin scale [12,13], have proclaimed small hydropower plants (SHPPs) and, particularly, the run-of-river (ROR) type as the new alternative. SHPPs have an installed capacity that usually varies from 0.1 to 10 MW, although this range may vary from country to country [14]; e.g., in Greece the max capacity is 15 MW. Small hydro (<10 MW) currently contributes over 40 GW of world capacity, with its potential estimated at more than 100 GW [15], while on a EU level the current overall installed capacity of SHPP is 19,699 MW, with Greece contributing 1.18% to this figure (232 MW of installed capacity) [16]. ROR SHPPs are installations with no water storage reservoir, except a small head pond capacity (a) directly constructed on the river or (b) diverting (by-pass) a small portion of the river's water, and all diverted water returns to the stream just below the powerhouse [17]. What is of particular importance is that ROR SHPPs can easily be constructed/adjusted to the left or right riverbanks of existing ROR irrigation dams, i.e., dams used for water stage elevation and diversion to adjoining canals; hence, a smaller environmental and social footprint is established. On the other hand, there is research questioning the eco-friendliness of small hydro [18].

Near-real-time data on produced energy on a EU scale, including hydropower from big HPPs, are available online by the European Network of Transmission System Operators for Electricity (ENTSO-E), with Skoulikaris and Krestenitis [19] proposing specific methodology for automatically retrieving energy datasets and then converting them to water discharge outflows; however, the ENTSO-E online repository does not include data from SHPPs that could further be exploited for research purposes. Various scholars have addressed issues related to the siting and sizing of small hydropower plants [17,20,21], operation optimization techniques and optimal design [22,23], and the contribution of ROR SHPPs on covering emerging energy demands [15,24,25]. Additional studies focused on identifying the costs of SHPP related to other energy sources [1], while others are concerned with the economics and maximization of the return on investment [26,27]. Moreover, although numerous studies have been performed on the operation of hydropower plants (HPPs) with storage capacities under climate change conditions [28–32], far fewer studies exist for large ROR HPPs [33,34]; while, to the author's knowledge, the investigation of climate change on run-of-river small hydropower plants is sparsely addressed within the literature. Kelly-Richards et al. [35], in whose research 248 articles were reviewed, among which 43 were related to ROR hydroplants, also concluded that low-head ROR SHPPs,

i.e., ROR plants without diversion structures, are not examined in terms of impacts in the literature.

Inspired by this literature gap, the research aims at proposing and implementing a specific methodology for run-of-river small hydropower plants, modelling under climate change conditions. For that purpose, two ROR SHPPs located in different water districts of Northern Greece are calibrated and validated with the use of a hydropower simulation model and, thereafter, are simulated under climate change conditions. The future river discharges used as input to the hydro plants' simulations come from a pan-European hydrological model, forced by three different Regional Climate Models under the 4.5 and 8.5 Representative Concentration Pathways for a short-term future (2031–2060) and a long-term future (2071–2100) period. Both the rivers' discharges and the generated energy outputs are compared to the relevant data of a reference period, to identify potential correlation patterns between the fluctuations of discharges and energy production and to analyze the behavior of the two hydrosystems under climate change. The applicability of the research to any ROR SHPPs on a European scale constitutes this contribution a useful methodological framework for assessing climate change at river basins, where water-energy-agriculture nexus schemes with SHPPs installations are prevailing.

## 2. Materials and Methods

### 2.1. Case Study Areas

The two SHPPs under investigation are located in Northern Greece but in different water districts (WD) with different hydroclimatic characteristics. The Gitani SHPP, hereinafter SHPP-A, is constructed on the Kalamas River, which is a national river located in the WD of Epirus (EL05) (northwestern Greece), Figure 1. The specific WD receives the highest annual precipitation volumes on a national scale, with the mean annual rainfall on the mountainous parts of the basin exceeding 2000 mm [36]. The Eleousa SHPP, hereinafter SHPP-B, is located on the Axios River approximately 28.0 km upstream of the river estuaries in the North Aegean Sea, Figure 1. The Axios River, which forms part of the transboundary Vardar/Axios River that is shared with North Macedonia (upstream country) and Greece (downstream country), belongs to the WD of Central Macedonia (EL10) (north-central Greece) with the annual rainfalls in this area ranging from 400–600 mm; hence, the river's runoff highly depends on the transboundary water inflows [37]. The main hydrological characteristics of the two rivers are depicted in Table 1 [38–40].

**Table 1.** Characteristics of the River Basins that supply the case study SHPPs with water.

River	WD	Length (km)	Basin Area (km <sup>2</sup> )	Mean Elevation (m)	Annual Precipitation (mm)	Seasonal Precipitation (mm) <sup>4</sup>				Annual Discharges (×10 <sup>6</sup> m <sup>3</sup> )	Averaged Seasonal Discharges (m <sup>3</sup> /s)			
						DJF	MAM	JJA	SON		DJF	MAM	JJA	SON
Kalamas	EL05	115	2523	544	1000–1200 (coastal area)	487.8	260.6	487.8	481.8	2049	92.8	55.8	8.7	46.4
					1800–2200 (mountainous area)									
Axios <sup>1</sup>	EL10	76	3327 <sup>2</sup>	180	400–600 (Greek part)	103.6	152.7	103.6	68.6	4400 <sup>3</sup>	143.2	206.3	84.6	75.9
					700 (North Macedonian part)									

<sup>1</sup> The provided figures are referred to as the Greek part of the basin. <sup>2</sup> It includes the extent of the Loudias River Basin according to the SSW 2013b. <sup>3</sup> The provided annual discharge volume reflects the inflows from North Macedonia ( $3600 \times 10^6 \text{ m}^3$ ) and the one drained in the Greek part of the basin ( $800 \times 10^6 \text{ m}^3$ ). <sup>4</sup> DJF: December-January-February, MAM: March-April-May, JJA: June-July-August, SON: September-October-November.

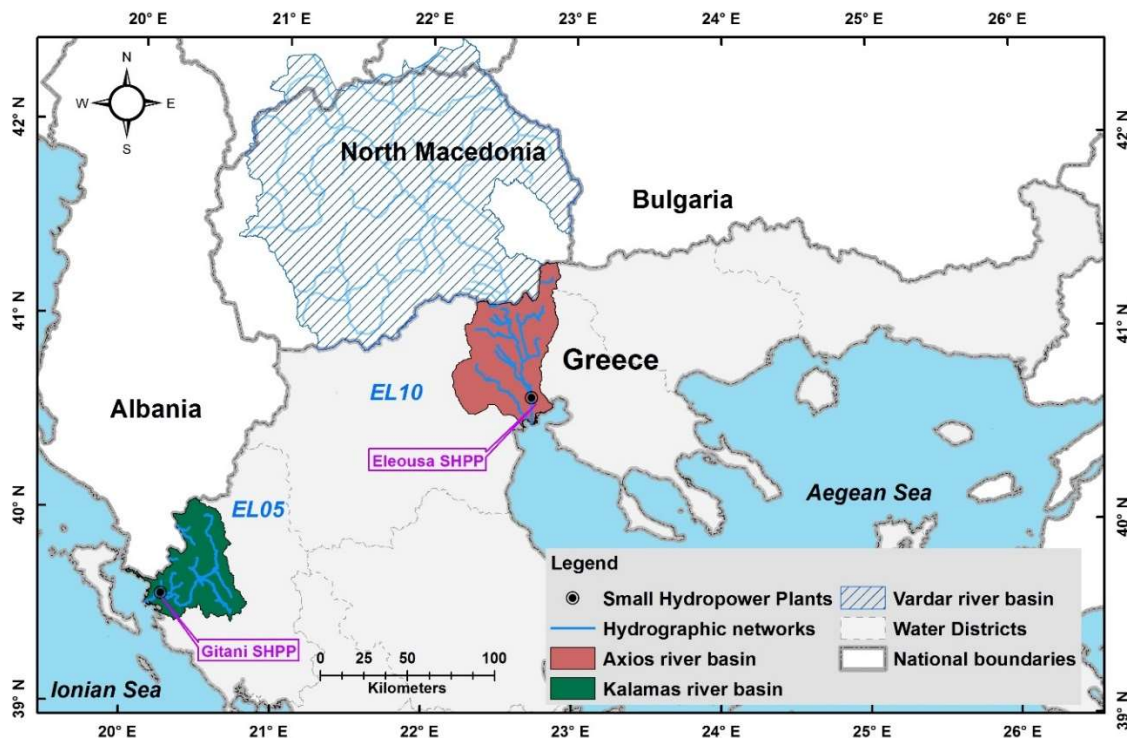


Figure 1. Case study SHPPs locations within the relevant river basins.

Both SHPPs were constructed on the right side of existing run-of-river irrigation dams that were built in the late 1950s and early 1960s, in order to elevate the rivers' water level and divert specific water volumes to adjoining irrigation channels. In both cases, the SHPPs make use of the elevation difference caused by the irrigation dams to satisfy the required hydraulic head for their operation, Table 2. The irrigation water, which equals  $5.25 \text{ m}^3/\text{s}$  and  $45.0 \text{ m}^3/\text{s}$  for SHPP-A and SHPP-B, respectively, is diverted from mid-April to the end of September (irrigation period), through irrigation channels located just upstream of the plants' intake structures, while no other important water abstractions occur during the rest of the year. The operation of the Gitani and Eleousa SHPPs were initiated in 2006 and 2008, respectively, with their technical characteristics presented in Table 2 [14,41].

Table 2. SHPPs technical characteristics.

SHPP	River	Capacity (MW) per Unit	No. of Units	Annual Produced Energy (GWh)	Turbines' Type	Max Water Discharges ( $\text{m}^3/\text{s}$ ) per Turbine	Min Discharges ( $\text{m}^3/\text{s}$ ) for Operation	Hydraulic Head (m)	Dams' Overflow Height (m)	Dams' Length (m)
Gitani	Kalamas	2.1	2	15.2	Kaplan	60	6.0	$\pm 7.12$	13.77	152
Eleousa	Axios	3.4	2	29.7	Kaplan	70	15.0	$\pm 5.68$	12.90	1170

## 2.2. Simulation of Hydropower Generation

The simulation of the SHPPs was implemented with the use of the Reservoir System Simulation model, the HEC-ResSim model (<https://www.hec.usace.army.mil/software/hec-ressim/>) (accessed on 17 June 2021) of the U.S. Army Corps of Engineers, Institute for Water Resources, Hydrologic Engineering Center (CEIWR-HEC) (Davis, CA, USA) [42]. The model simulates reservoir operations for flood and water resources management, low flow augmentation, and water supply as well as hydropower production, either for detailed operational plan investigations or real-time decision support [43]. The model represents large- and small-scale reservoir systems through a network of elements (junctions, routing reaches, diversions, reservoirs) that are customized defined by the modeler. What is of

particular importance is that the model can simulate both single events and long-term operation using available time-steps.

HEC-ResSim consists of three main modules: the watershed setup, the reservoir network, and the reservoir simulation [42]. Within the watershed setup, the schematization of the hydrographic network together with the structural elements consisting of the hydrosystem, such as reservoirs, diversions, levees, and gauge location, are defined. The technical (e.g., the dam's crest elevation and height, the number and type of turbines, the spillways characteristics, etc.) and operational (e.g., operation schedule of power plant, elevation-related decisions, designation of flood control, conservation and inactive zones, etc.) characteristics of the elements are specified within the reservoir network module. Potential various operational alternatives, such as the use of one or two turbines for specific inflows and scenarios related to the input flows, are also defined within this module. Finally, the reservoir simulation module is the interface for defining the simulation time and computation interval for simulating the produced alternatives and scenarios. As denoted in the literature, HEC-ResSim has successfully been applied in various time scales and case studies, both for current and climate change conditions [44–50].

### 2.3. Watershed Hydrologic Simulations

The Kalamas and Axios Rivers' discharges were derived from the Hydrological Predictions for the Environment (HYPE) semi-distributed basin model [51], and, particularly, from the European version, i.e., E-HYPEv3.1.1, of the model [52]. E-HYPE simulates river flow generation from rainfall distribution and temperature by dividing the European territory at 35,408 catchments of mean size of 215 km<sup>2</sup>, and by taking into consideration the topography, the soil and land use characteristics, the irrigation and crop demands on water, the snow coverage, and the evapotranspiration at each catchment [52]. The applicability of the model for present, as well as climate change, conditions is peer reviewed in the literature [53–57]. In the research, simulated historical daily discharges from 1981 to 2010 (<https://hypeweb.smhi.se/explore-water/historical-data/europe-time-series/>) (accessed on 10 May 2021) and discharges under climate change conditions (<https://hypeweb.smhi.se/explore-water/climate-change-data/europe-climate-change/>) (accessed on 15 May 2021) were retrieved by E-HYPE's online data repository for (a) validation of the E-HYPE hindcast simulations against the rivers' gauged discharges and (b) assessment of the SHHPs' operation under climate change conditions.

### 2.4. Climate Change Datasets

The climatic parameters, used as forcing for the hydrologic model, are attributed to three high-resolution Regional Climate Models (RCMs) with a spatial resolution of 0.11 corresponding to 12.5 km grid spacing. All utilized RCMs, Table 3, have been developed and implemented in the framework of the Coordinated Regional Climate Downscaling Experiment for the European domain (Euro-CORDEX) [58]. The evaluation of climate change on the SHPPs' future power production was conducted for the Representative Concentration Pathways (RCPs) RCP4.5 and RCP8.5 and for the future periods 2031–2060 (hereinafter Short-Term Future (STF)) and 2071–2100 (hereinafter Long-Term Future (LTF)). RCP4.5 corresponds to stabilization of radiative forcing after the 21st century at 4.5 W/m<sup>2</sup> and represents a “moderate” future climate, while RCP8.5 poses a “worst case scenario” where rising radiative forcing crosses 8.5 W/m<sup>2</sup> at the end of 21st century [59]. Finally, to interpretate the future climatic variability in comparison to the past, the RCMs hindcasts for the reference period 1971–2000 (hereinafter REF) and the resulting river discharges were also used.

**Table 3.** Regional Climate Models utilized to trigger the hydrologic simulations and the future hydropower production in the case study areas.

RCM	Global Model	Institute	RCMs Short Description
CSC-REMO2009	MPI-M-MPI-ESM	MPI-Max Planck Institute for Meteorology Climate Service Center, Hamburg, Germany	It is a limited-area three-dimensional atmospheric circulation model based on the ‘Europa-Modell’ of the German Weather service and on the physical parameterizations of the global three-dimensional atmospheric circulation model ECHAM-4 [60].
KNMI-RACMO22E	EC-EARTH	KNMI-Royal Netherlands Meteorological Institute, De Bilt, the Netherlands	It combines the dynamical core of the High Resolution Limited Area Model (HIRLAM) numerical weather prediction model with the European Centre for Medium-range Weather Forecasts (ECMWF) Integrated Forecast System (ISF) physics [61].
SMHI-RCA4	HadGEM2-ES	SMHI-Swedish Meteorological and Hydrological Institute, Norrköping, Sweden	It is originally based on the numerical weather prediction model HIRLAM, and in the current version all data used for a simulation are read from globally valid physiography databases [62].

### 3. Results

#### 3.1. Hydropower Model Calibration and Validation

SHPPs were calibrated and validated against measured produced power, with gauged discharges upstream of the plants to be used as input data while the technical characteristics of the plants and their operational schedule were obtained by the SHPPs’ management authorities. The calibration and validation of both SHPPs were conducted for the periods 2015–2018 and 2019–2020, respectively.

Focusing on SHPP-A, a high degree of correlation between measured and simulated power during the calibration (Pearson correlation coefficient (PCC) = 0.917, Nash–Sutcliffe efficiency coefficient (NSE) = 0.798, coefficient of determination ( $R^2$ ) = 0.841, and Root Mean Square Error/max measured power (RMSE/max) = 14.01%) and validation (PCC = 0.916, NSE = 0.794,  $R^2$  = 0.839 and RMSE/max = 15.07%) phases was obtained, as depicted in Figure 2a. Regarding SHPP-B, a similar good performance was also achieved during the calibration (PCC = 0.851, NSE = 0.592,  $R^2$  = 0.723 and RMSE/max = 16.61%) and validation (PCC = 0.838, NSE = 0.355,  $R^2$  = 0.731, and RMSE/max = 17.05%) periods, as demonstrated in Figure 2b. In SHPP-A, as proved by the correlation coefficients, the simulated power follows the same trend with the measured one, with the occurrence of maximum and minimum power production in March and August, respectively, at interannual scale, to be successfully captured by the hydropower model. Moreover, maximum and minimum measured power values are accurately simulated by HEC-ResSim, since the mean deviation between simulated and measured maximums equals 0.10 MW and 0.16 MW, and the mean deviation for the minimums equals 0.04 MW and 0.02 MW for the calibration and validation periods, respectively. In SHPP-B, the maximum power production does not follow a clear pattern, with the maximums to be presented either in November or December or March or May. The simulated power, nevertheless, successfully captures this dissimilarity, with the mean deviation between measured and simulated maximums being 0.17 MW and 0.19 MW for the calibration and validation periods, respectively.

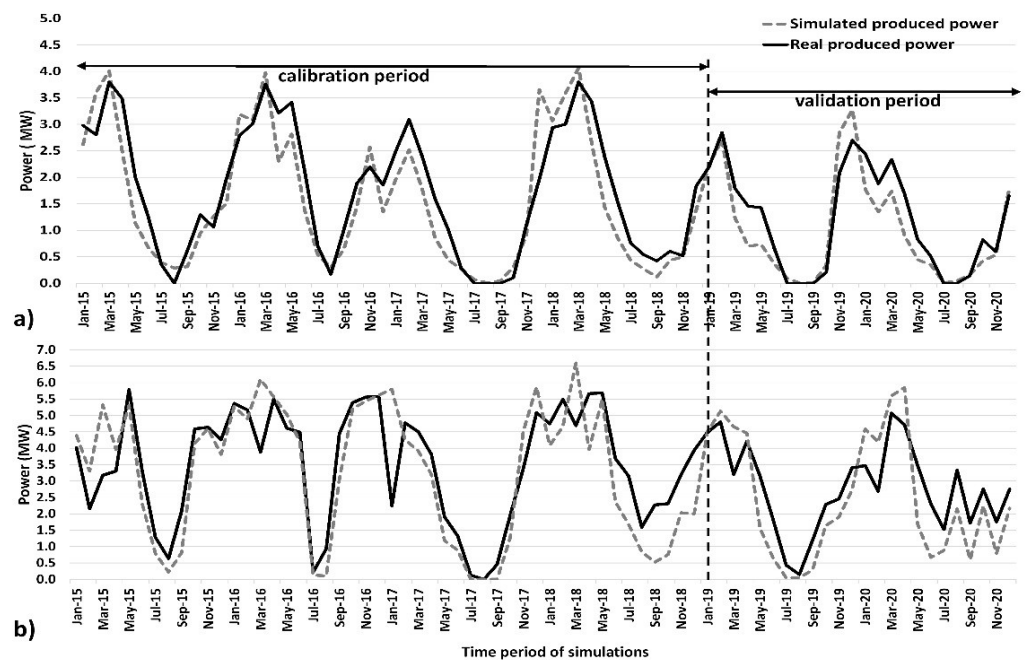


**Figure 2.** HEC-ResSim model calibration and validation produced power outputs in comparison to measured power data for (a) SHPP-A (Gitani) and (b) SHPP-B (Eleousa).

### 3.2. Validation of Hydrological Model on the Case Study Basins

To use the E-HYPE hydrological model for the simulation of the river discharges under the various climate models and scenarios, the a priori validation of the model's behavior on the Kalamas and Axios Rivers was initiated. For this purpose, the available historic runoff simulation outputs derived by the hydrological model and based on observed precipitation and temperature datasets covering Europe, as well as on streamflow data from the European Water Archive (EWA) and the Global Runoff Data Base (GRDB) [63], were retrieved by the E-HYPE online repository for the two case study rivers covering a period of 30 years, i.e., from 1981 to 2010. However, for the Kalamas River, continuous gauged discharges exist from 2007 till currently, while continuous flow measurements on the Axios River are available for the period 1971–1990 and from 2010 till currently. Hence, the evaluation of E-HYPE model on simulating the Kalamas and Axios Rivers was conducted for the periods 2007–2010 and 1981–1990, respectively, with the outputs to be illustrated in Figure 3a,b.

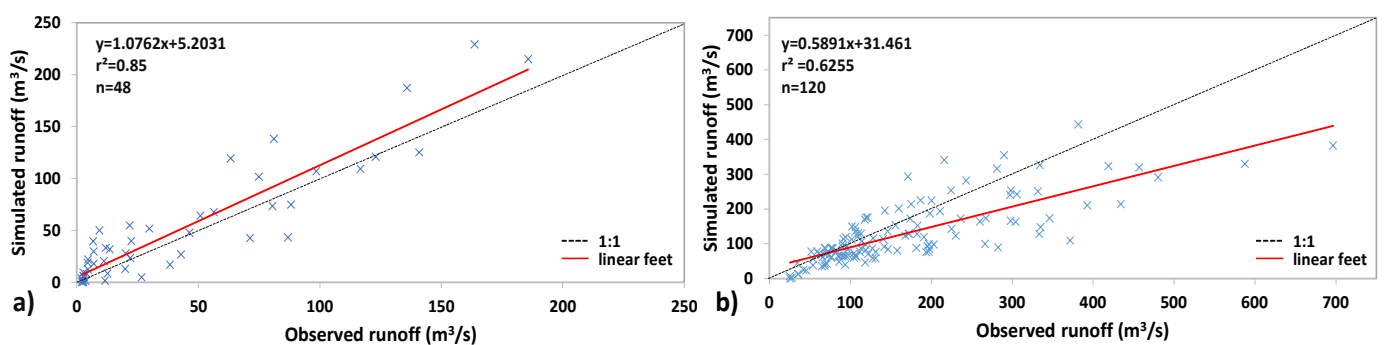


**Figure 3.** Validation of the E-HYPE model's historic runoff simulations against gauged data on (a) the Kalamas River for the period 2007–2010 ( $n = 48$  months) and (b) the Axios River for the period 1981–1991 ( $n = 120$  months).

In the case of the Kalamas River, the implemented goodness of fit tests (PCC = 0.922, NSE = 0.829,  $R^2 = 0.850$ , and RMSE/max = 10.28%) demonstrates the high accuracy of

the E-HYPE model in simulating the runoff. The implemented indices for the Axios River ( $PCC = 0.791$ ,  $NSE = 0.378$ ,  $R^2 = 0.625$  and  $RMSE/\max = 18.45\%$ ), although less high than the one of the Kalamas River mainly due to its large extent and its transboundary nature, also designated the ability of the hydrological model to represent the river discharges. Especially, the fact that  $RMSE/\max$  in both cases is less than  $20.0\%$ , a figure that is considered relatively low, together with the high correlation figures supports the further utilization of the model with forcing by climate change models.

### 3.3. River Discharges under Climate Change

The simulation of the rivers' discharges under climate change derived from the E-HYPE hydrological model triggered by the CSC-REMO2009, KNMI-RACMO22E, and SHMI-RCA4 RCMs under the RCP4.5 and RCP8.5 climatic scenarios for the STF (2031–2060) and LTF (2070–2100) periods, respectively. Hindcast rivers' discharges, also coming from the forcing of the hydrological model by the three RCMs' hindcast variables, covering the reference period (REF) 1971–2000, were used for the assessment of the future rivers' runoff fluctuations. The outputs of the simulations are presented in Figure 4.

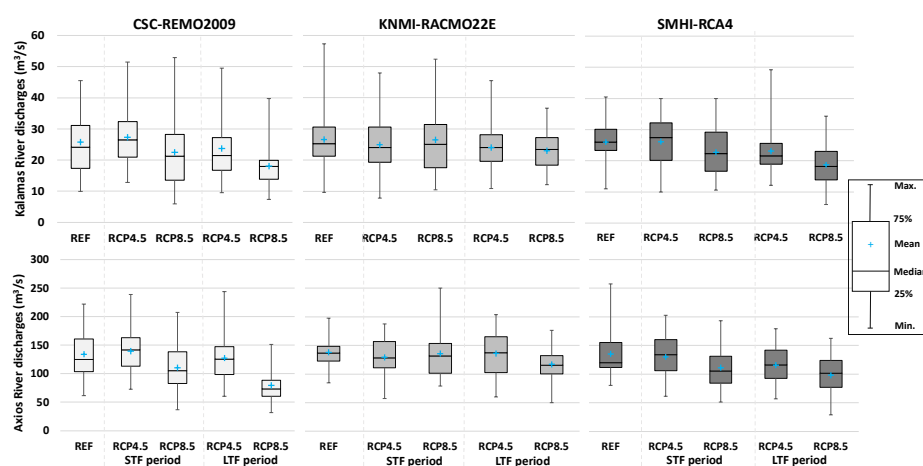


**Figure 4.** Runoff characteristics of the Kalamas (first row of boxplots) and Axios (second row of boxplots) Rivers under climate change conditions, with the hydrologic simulations to be forced by the CSC-REMO2009 (light grey boxplots), KNMI-RACMO22E (grey boxplots), and SHMI-RCA4 (dark grey boxplots) RCMs for the STF (2031–2060) and LTF (2071–2100) periods, in comparison to the REF (1971–2000) period.

In the Kalamas River, where the SHPP-A is located, the ensemble discharges for the REF period, i.e., the averaged mean discharges derived by the forcing of E-HYPE with the three RCMs' hindcasts, equal  $26.15 \text{ m}^3/\text{s}$  with a mean deviation of  $\pm 0.29 \text{ m}^3/\text{s}$ . For the STF period and the RCP4.5 scenario, forcing by the REMO2009 model present a small discharges' increase of up to  $5.9\%$  (in comparison to the REF period), the outputs for the RACM022E model demonstrate a decrease of  $6.3\%$ , while the outputs attributed to RCA4 show no alterations in the mean discharges, shown in Figure 4 and Table 4. For the same climatic scenario but for the LTF period, discharges' decrease of  $12.7\%$  are presented for both the REMO2009 and RCA4 models' simulations, while those produced by inputs of the RACM022E model demonstrate a negligible decrease of  $0.5\%$ . On the other hand, the outputs for the RCP8.5 scenario are more homogeneous. Particularly, for the STF period the ensemble discharges' reduction is  $9.67\%$ , with the mean deviation among the simulations' outputs equal to  $\pm 1.08 \text{ m}^3/\text{s}$ . For the LTF period, significant discharges reduction of around  $30\%$  are presented for both the REMO2009 and RCA4 models' simulations, while an important but less severe decline of  $13.4\%$  is forecasted for the simulations forced by the RACM022E model.

**Table 4.** The Kalamas and Axios Rivers simulated discharges ( $\text{m}^3/\text{s}$ ) and differences (%) with the REF period per RCP and time periods under the three RCMs.

River	Model Forcing By	Discharges ( $\text{m}^3/\text{s}$ ) Per RCPs/Time Period					% Difference with REF Per RCPs/Time Period				
		Historical/REF	4.5/STF	4.5/LTF	8.5/STF	8.5/LTF	Historical/REF	4.5/STF	4.5/LTF	8.5/STF	8.5/LTF
Kalamas	REMO2009	25.84	27.37	22.53	23.72	18.06	0	5.9	−12.8	−8.2	−30.1
	RACMO22E	26.59	24.92	26.54	24.05	23.02	0	−6.3	−0.2	−9.5	−13.4
	RCA4	26.02	26.15	22.76	23.09	18.73	0	0.5	−12.6	−11.3	−28.0
Axios	REMO2009	134.06	139.34	110.46	127.19	79.35	0	3.94	−17.60	−5.12	−40.81
	RACMO22E	137.98	129.40	135.80	135.94	116.86	0	−6.22	−1.58	−1.48	−15.31
	RCA4	135.08	129.96	111.17	115.63	98.05	0	−3.79	−17.70	−14.40	−27.41

In the case of the river where SHPP-B is located, i.e., the Axios River, the ensemble discharges for the REF period are  $135.70 \text{ m}^3/\text{s}$  with a mean deviation of  $\pm 1.52 \text{ m}^3/\text{s}$ . A slight increase of 3.94% of the river discharges is only presented for one model and one scenario, i.e., for the REMO2009 model under the RCP4.5 for the STF period, while in all other combinations of models and scenarios a decline of the future river's runoff is projected. Particularly, for the RCP4.5 and the STF period, the simulations for both the RACMO22E and RCA4 models show discharges' decreasing from 3.79% to 6.22%, while for the LTF period the reduction of the discharges is 17.65% for the REMO2009 and RCA4 models, respectively, and around 2.0% for the RACMO22E model, as shown in Figure 4 and Table 4. The most severe river discharge's declines are projected for the RCP8.5 scenario and the LTF period, where the ensemble discharges equal  $98.08 \text{ m}^3/\text{s}$ , i.e., 27.73% less than the ensemble ones of the REF period. Focusing on each RCM model separately, decreases of 40.81%, 15.32%, and 27.40% are foreseen when the simulations forced by the REMO2009, RACMO22E, and RCA4 models, respectively, for the later climatic scenario and simulation period.

In terms of intermonthly variations of the river discharges for the 30-year periods, Figure 5, data analysis showed that for the Kalamas River and the simulations forced by the REMO2009 climatic model, Figure 5a, a significant decrease in the river's runoff for both the STF and LTF periods and both climatic scenarios is apparent in February (at least  $<10.0 \text{ m}^3/\text{s}$  compared to the REF period, i.e.,  $\sim 22.1\%$  discharges' reduction), in April ( $\sim 24.8\%$  discharges' reduction), and in June–July–August ( $\sim 26.21\%$  discharges' reduction). Moreover, apart from the RCP4.5 scenario and the STF period (light grey-colored column bars of Figure 5) where discharges' increases are observed during various months, e.g., in January, March, October, November, and December, the outputs for the RCP8.5 scenario as well as the STF and LTF periods (bars with horizontal stripes and black-dotted bars of Figure 5, respectively) indicate runoff decreases in almost all months. Simulations related to the RACMO22E model, Figure 5b, demonstrate that the discharges' decrease occurs mainly from September to November (mean decrease for both climatic scenarios and both simulation periods equals  $\sim 33.6\%$ ), while from January to May the projected increases of the river runoff depends on the climatic scenario and simulation period, e.g., in March the runoff increase equals 18.47% and 0.2% for the STF and LTF periods under the RCP8.5 scenario, respectively. Discharges simulations triggered by the RCA4 climate model, Figure 5c, revealed that the most significant discharges reductions occur in February (at least 9.6% regardless the simulation period and scenario), in October ( $\sim 18.5\%$ ), and in December (mean discharge reduction of 26.0%). On the other hand, from March to May, the variation between the future discharges and the REF period is negligible.

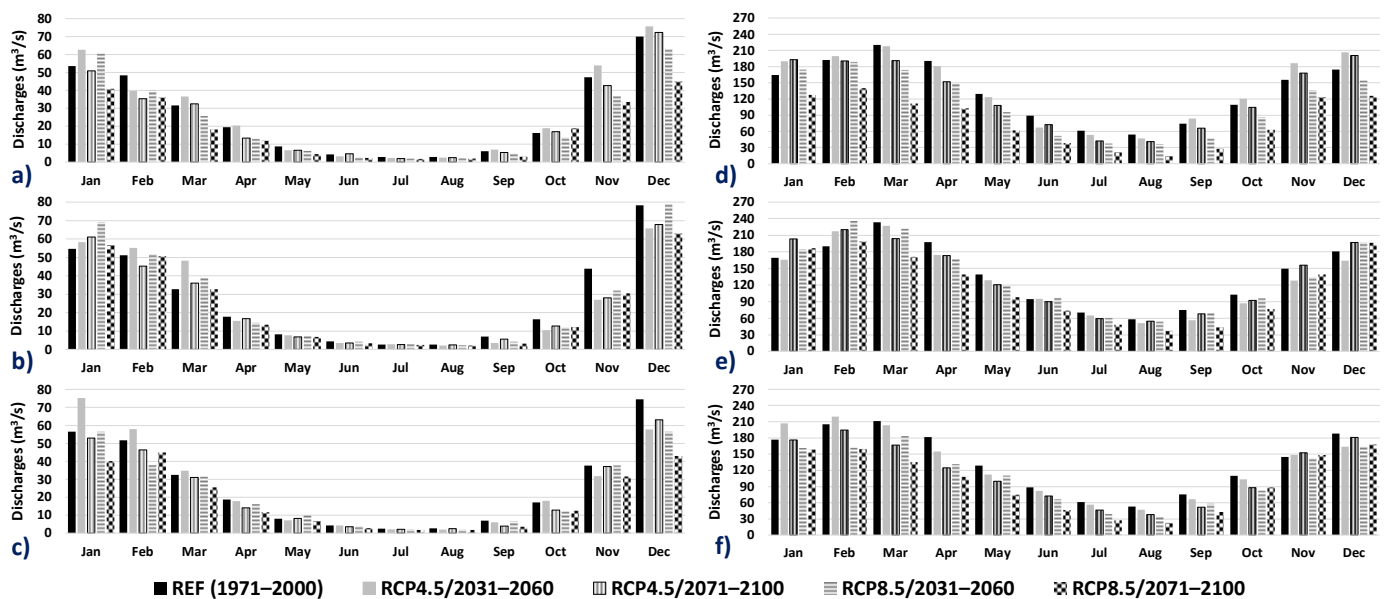


**Figure 5.** Intermonthly discharge variations of the Kalamas River (a–c) and of the Axios River (d–f) for the evaluated 30-year periods, where the black-colored bars correspond to the REF periods, the light-gray columns to the RCP4.5 scenario and the STF periods, the bars with the vertical stripes to the RCP4.5 scenario and the LTF periods, the bars with the horizontal stripes to the RCP8.5 scenario and the STF period, and the black-dotted bars to the RCP8.5 and the LTF periods of each RCM, respectively. (a,d) Attribute the hydrologic simulations forced by the REMO2009 model, (b,e) the ones forced by the RACMO22E model, and (c,f) the ones forced by the RCA4 model.

In the Axios River, where the river discharges are quite bigger than those of the Kalamas River, the simulations attributed to the REMO2009 model, Figure 5d, showed that for the RCP4.5 scenario, regardless the simulation period, the simulated river discharges are bigger than those of the REF period for January to February and from October to December. The higher decreases in the same scenario are presented from May to August. In all cases, the simulations corresponding to the RCP8.5 and the LTF period are at least 22.3% lower than those of the REF period, while in June, July, and August the discharges decrease from  $89.2 \text{ m}^3/\text{s}$  to  $38.2 \text{ m}^3/\text{s}$  (~57.1% reduction), from  $61.01 \text{ m}^3/\text{s}$  to  $21.32 \text{ m}^3/\text{s}$  (~65.0% reduction), and from  $54.11 \text{ m}^3/\text{s}$  to  $14.45 \text{ m}^3/\text{s}$  (73.3% reduction), respectively. As depicted in Figure 5e, which corresponds to forcing by the RACMO22E model, regardless of the scenario and simulation period the larger monthly runoff decline does not exceed 20.0% in comparison to the REF period, while during the winter, i.e., from December to February, all the outputs demonstrate runoff augmentation at least of 9.4%, in comparison to the REF period. A clear reduction of the discharges varying from 15.0% to 20.0% is only presented from July to September for all the scenarios and both the STF and LTF periods. Finally, and regarding the RCA4 model, Figure 5f, a clear decreasing trend of river discharges varying from 18.5% to 33% is noted from March to September, while November is the only month when no runoff reduction is observed. During the winter months, the simulations related to the RCP8.5 and the STF period are approximately the same as those of the LTF period, e.g., in February, the reductions of 22.1% and 21.0% are presented for the LTF and STF periods, respectively, compared to the REF period. On the other hand, and for the same climatic scenario, during the summer months the discharges linked to the LTF period are much smaller than those of the STF period, e.g., in August reductions of 57.2% and of 27.3% are presented for the LTF and STF periods, respectively, compared to the REF period.

### 3.4. Energy Generation Projections

The analysis of SHPP-A future-generated energy demonstrated a clear decreasing trend in comparison to the REF period. In terms of absolute values, the larger mean energy

decrease for the 30-year periods of 2.56 GWh is depicted by the simulation driven by the REMO2009 model, followed by a decrease of 2.28 GWh attributed to the RCA4 model. In case of the simulations forced by the RACMO22E model, the maximum 30-year mean energy reduction is up to 0.75 GWh, as shown in Table 5. Moreover, as depicted in Table 5, the HEC-ResSim simulations attributed to the REMO2009 model show an escalating energy reduction of 9.25% for the RCP4.5 scenario and the LTF period, and of 16.70% and 25.79% under the RCP8.5 scenario and the STF and LTF periods, respectively, when compared to the REF period. The only case that an energy increase is foreseen is attributed to the RCP4.5 scenario and the STF period, with this small increase of 3.28% connected to the aforementioned discharges' increase (see Section 3.3) that was found for the same scenario and simulation period. For the simulations triggered by the RACMO22E model, the larger energy decreases of 7.57% and 7.55% are presented for the STF period under the RCP4.5 and RCP8.5 scenarios, respectively. On the other hand, for the LTF period the simulated energy reduction is approximately 2.85% for both climatic scenarios. As for the outputs connected with the RCA4 climatic model, the larger energy declines are related with the LTF period, i.e., decreases of 12.03% and 21.97% for the RCP4.5 and RCP8.5 scenarios, respectively. For the STF period, the larger energy diminution of 10.31% is presented under the RCP8.5 scenario, while for the RCP4.5 scenario the relevant decrease of 1.56% is much smaller.

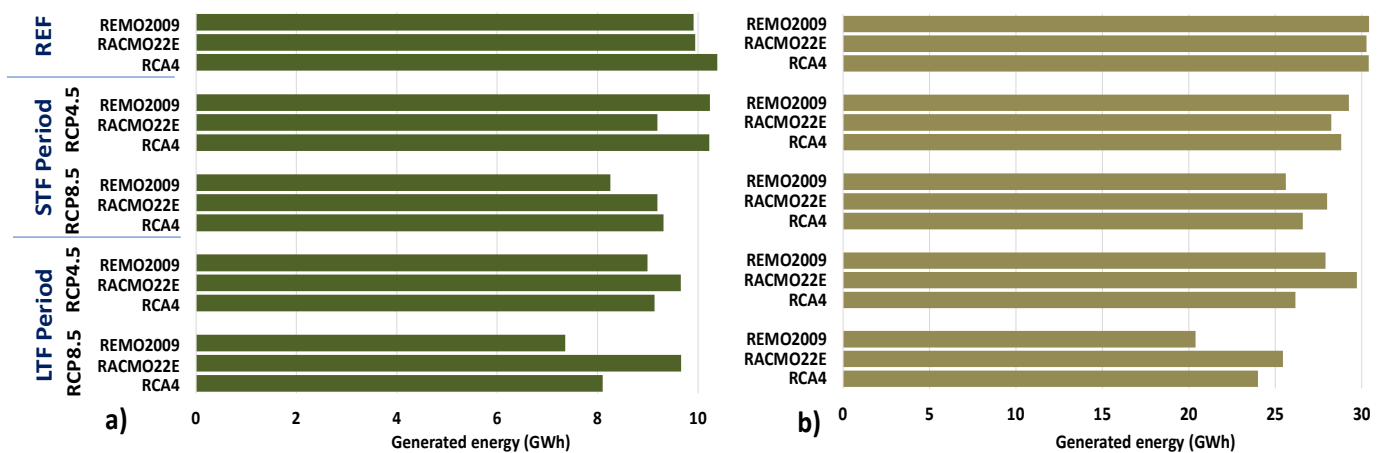
**Table 5.** HEC-ResSim model results of mean produced energy (GWh) and of differences (both in GWh and %) between historical and future energy generation by different forcing inputs as REMO2009, RACMO22E, and RCA4 for the SHPP-A.

Scenario	Period	Mean Produced Energy (In GWh)			Difference with REF (In GWh)			% Difference with REF		
		Forcing by REMO2009	Forcing by RACMO22E	Forcing by RCA4	Forcing by REMO2009	Forcing by RACMO22E	Forcing by RCA4	Forcing by REMO2009	Forcing by RACMO22E	Forcing by RCA4
Historical	REF	9.91	9.94	10.38	0	0	0	0	0	0
RCP4.5	STF	10.23	9.19	10.22	0.32	−0.75	−0.16	3.28	−7.57	−1.56
RCP4.5	LTF	8.99	9.66	9.13	−0.92	−0.28	−1.25	−9.25	−2.86	−12.03
RCP8.5	STF	8.25	9.19	9.31	−1.66	−0.75	−1.07	−16.70	−7.55	−10.31
RCP8.5	LTF	7.35	9.66	8.10	−2.56	−0.28	−2.28	−25.79	−2.84	−21.97

Focusing on the SHPP-B case study, the simulation outputs revealed an important lessening of the future produced energy, especially for the LTF period (2071–2100) of the RCP8.5 climatic scenario, as shown in Table 6. Particularly, the mean energy production of 30.41 GWh of the REMO2009 model's REF period is projected to be 20.38 GWh, i.e., a decrease of approximately 33.0%; the 30.27 GWh of the RACMO22E model's REF period is projected to reach 25.43 GWh, i.e., ~16% decrease, while the 30.41 GWh that were simulated with forcing by the RCA4 model will equal to 24.00 GWh, i.e., a decrease of ~21.0%. A more detailed view of the figures of Table 6 shows that the energy production associated to the REMO2009 model presents an escalating decrease, i.e., for the STF period the decrease equals 3.82% and 15.81% for the RCP4.5 and RCP8.5 scenarios, respectively, while for the LTF period the decrease is more than doubled (8.26% and 32.98% for the RCP4.5 and RCP8.5) than the relevant one of the STF period. Regarding the RACMO22E model, for the STF period the projected reduction varies between 6.74% and 7.51%, as shown in Table 6, while for the LTF period a negligible energy reduction of 1.80% is projected under the RCP4.5 scenario, and a rather significant reduction of 15.98 is foreseen under the RCP8.5 scenario. Finally, the outputs produced by the forcing of the HEC-ResSim model with river discharges attributed to the RCA4 model, show that under the STF period the energy decline is up to 5.28% and 12.53% for the RCP4.5 and RCP8.5 scenarios, respectively, and under the LTF period these figures reach up to 13.97% and 21.06% for the same climatic scenarios, respectively. A graphical representation of the mean produced energy for all the examined models, scenarios, and time periods (30 simulations in total) is given in Figure 6, where the important lessening of the future produced energy associated to the LTF period and the RCP8.5 scenario is clearly depicted for both SHPPs.

**Table 6.** HEC-ResSim model results of mean produced energy (GWh) and of differences (both in GWh and %) between historical and future energy generation by forcing different inputs as REMO2009, RACMO22E, and RCA4 for the SHPP-B.

Scenario	Period	Mean Produced Energy (In GWh)			Difference with REF (In GWh)			% Difference with REF		
		Forcing by REMO2009	Forcing by RACMO22E	Forcing by RCA4	Forcing by REMO2009	Forcing by RACMO22E	Forcing by RCA4	Forcing by REMO2009	Forcing by RACMO22E	Forcing by RCA4
Historical	REF	30.41	30.27	30.41	0	0	0	0	0	0
RCP4.5	STF	29.25	28.23	28.80	−1.16	−2.04	−1.61	−3.82	−6.74	−5.28
RCP4.5	LTF	27.90	29.72	26.16	−2.51	−0.54	−4.25	−8.26	−1.80	−13.97
RCP8.5	STF	25.60	27.99	26.60	−4.81	−2.27	−3.81	−15.81	−7.51	−12.53
RCP8.5	LTF	20.38	25.43	24.00	−10.03	−4.84	−6.40	−32.98	−15.98	−21.06

**Figure 6.** Schematic representation of the future generated energy under the STF and LTF periods for the RCP4.5 and RCP8.5 climatic scenarios, as well as the generated energy in the REF period for (a) the Gitani SHPP (SHPP-A) and (b) the Eleousa SHPP (SHPP-B).

#### 4. Discussion

The modeling and simulation of ROR SHPPs located in rivers with different hydrologic characteristics under various climate change models and scenarios, as well as different time frames, forms the subject of the research. The current contribution sheds light on this thematic area, which is negligibly addressed within the literature. The proposed methodology, i.e., the coupling of freeware hydropower simulation models (e.g., the HEC-ResSim model) with large scale hydrologic models (e.g., the E-HYPE model) and big-data simulations (e.g., the Euro-CORDEX climate data), is also conceived as an innovative part of the research, which can be applied to numerous case studies on the European scale. Finally, the simulation of the two case study SHPPs is conducted for the first time, and the energy and river discharges' outputs can be assessed both on the regional and national level for the sustainable management of the hydrosystems under investigation.

##### 4.1. Interpretation of Findings

The research, amongst others, investigates the impact of climate change on the Kalamas and Axios hydrosystems, an issue that is rather limited in its address within the literature. Focusing on the Axios River, very few scholars are identified to have worked on the thematic of water resources and climate change, e.g., Kapetas et al. [64] evaluated the way that climate change (use of CMIP5 climate model under the RCP4.5 scenario), by altering the river flow and precipitation patterns, could affect the coastal aquifers of the Axios basin in terms of salinization, or Poulos et al. [65] assessed the consequences of future sea-level rise (by using two customized scenarios of 1.0 and 0.5 m of sea-level rise) on the coastal plain of the Axios River. At the upstream part of the Axios River in North Macedonia (aka the Vardar River) there exists relevant literature; exceptions are Monevska [66], demonstrating precipitation and runoff decreases of 13.0% and 18.8%, respectively, by 2100 based on averaged ensemble values from four General Circulation

Models (CSIRO/Mk2, HadCM3, ECHAM4/OPYC3, NCAR-PCM) scaled to six emission scenarios (SRES A1T, A1Fl, A1B, A2, B1, and B2) and Granados et al. [67], where the averaged values of the utilized Water Availability and Adaptation Policy Analysis (WAAPA) model triggered by eight model runs for the A2 scenario, four model runs for the B2 scenario, three model runs for the A1B scenario, and five model runs for each RCP-2, RCP-4, RCP-6 and RCP-8 scenario, demonstrated a decrease in the Vardar/Axios's river runoff of 23.0%. For the Kalamas River, despite its importance at regional scale, apart from the Regional Adaptation Action Plans to climate change [68] where a vulnerability analysis for various environmental sectors, economic, and social activities is conducted, no relevant scientific publications were identified.

The current research demonstrates that although future discharges' decreases are foreseen for both rivers, the projected reduction is larger in the Axios River than in the Kalamas River, especially under the RCP8.5 climatic scenario, as shown in Figure 4 and Table 4. In both river basins and under the RCP4.5 scenario and the STF period (2031–2060), a small raise of the runoff (varying from 3.94% to 5.9%) is presented for the REMO2009 model; however, this is the only combination of models-scenarios-simulation period that a discharges increase is presented. The simulations linked to the same model demonstrate that the larger impacts are presented during the LTF period (2071–2100), where the decrease in the Kalamas River discharges equals 12.8% and 30.1% and the decrease in the Axios River discharges equals 17.6% and 40.81% for the RCP4.5 and RCP8.5 scenarios, respectively. In both cases, the figures demonstrate a more-than-double runoff decrease when the RCP8.5 climatic scenario is applied. Research on the Drin Basin, which is in proximity with the two case study basins, validates the current outputs, since Papadaki and Dimitriou [69] concluded that the discharges trend slope expressed in percent per year equals  $-0.14\%$  and  $-0.5\%$  under the REMO2009 RCP4.5 and RCP8.5 simulations, respectively. In case of the E-HYPE simulations triggered by the RACMO22E model, the outputs are very similar in both rivers for the RCP4.5 scenario, i.e., runoff reduction of about 6.3% for the STF period and runoff reduction  $< 1.6\%$  for the LTF period; while for the worst-case scenario (RCP8.5/LTF), the projected discharge decline is approximately 15.0% for both rivers in comparison to the REF period. Likewise, less severe results of climate change on water resources attributed to the RACMO22E model are also presented in the literature [70,71]. As far as the simulations connected to the RCA4 climatic model are concerned, the discharges are projected to decrease less than 3.79% and about 12.6–17.7% for the STF and LTF periods, respectively, under the RCP4.5 scenario for both rivers. Under the RCP8.5 scenario, a doubling of the runoff decrease is foreseen between the STF and LTF periods, e.g., in the Axios River the STF simulated runoff decrease of 14.4% turns to 27.41% for the LTF period; this is an argument about the model predictions that is supported by the literature [69].

An additional contribution from the research is the simulation of ROR small hydropower plants under climate change conditions. The projected rivers' runoff decrease is bound to have direct impact on the SHPPs energy production. As depicted in Table 5, for the SHPP-A case study the larger energy decreases of 25.79% and 21.97% are connected to the REMO2009 and RCA4 models, respectively, for the RCP8.5/LTF. For the same models and the RCP4.5/LTF, the maximum energy reduction is projected to be  $\sim 12.0\%$  in comparison to the REF periods. For the RCP8.5/STF combination of simulations, the only case where the energy decrease will be bigger than 15.0% is attributed to the REMO2009 model (reduction of 16.7%), while the other two models show a much smoother reduction (max reduction of  $\sim 10.0\%$ ). It should be noted that all the simulations forced by the RACMO22E model demonstrate small energy production lessening (up to  $\sim 7.5\%$ ). For the SHPP-B case study, the results in Table 6 show that the most important impacts on hydroelectricity generation are connected to the RCP8.5/LTF simulations, with the projected decrease to equal  $\sim 33.0\%$ ,  $\sim 16.0\%$ , and  $\sim 20.0\%$  for the REMO2009, RACMO22E, and RCA4 models, respectively. The second-largest impacts, in terms of energy production, are also linked to the RCP8.5 scenario but for the STF period, where the energy decrease will be approxi-

mately half (Table 6) the one simulated for the LTF period. For the RCP4.5 scenario and the LTF period, although representing the end of the 21st century where the most severe impacts are anticipated, the reduction of energy generation is less important (or almost equal for the RCA4 model) than the one simulated in the RCP8.5/STF.

An important output of the research is the connection between the produced energy of ROR SHPPs and river discharges as well as the role of runoff's intermonthly distribution and occurrence. As expected, large discharges' decreases are linked to significant reductions of energy generation, e.g., a 30.1% decrease in the Kalamas River's discharges coincides (Table 4) with an energy decrease of 25.79%, and a 40.81% decrease in the Axios River's discharges matches with an energy reduction of 32.98% under the REMO2009/RCP8.5/LTF simulations (Tables 5 and 6). However, the detailed analysis of the results demonstrated that this is not always the case, i.e., there is not an analogical pattern between river discharges and energy reductions because there are cases where quite big discharges' decreases coincide with small energy reduction, or small discharge declines cause large energy generation lessening. For example, in the Kalamas River and the simulations related to RACMO22E/RCP8.5/LTF, discharges' decrease of 13.4% causes an energy reduction of 2.84%, or, on the contrary, in the Axios River and the simulations related to REMO2009/RCP8.5/STF, discharges' decrease of 5.12% causes an energy decline of 15.81%. This non-correlation between river discharges and generated energy is due to the structural elements of run-of-river small SHPs, where the lack of reservoir for water stockage does not permit water releases from the reservoir in low flow periods [22] and, due to the unpredictable seasonality of the river discharges [72], even at the monthly level. The latter means that if the decrease of an important river's discharges occurs during periods of high flows (usually from November to March for Mediterranean rivers [73]), the available water volumes still cover the hydropower demands and the SHPPs' generated energy is slightly affected. The monthly distribution of the runoff triggered by the RACMO22E model (Figure 5b,e) validates this argument, particularly for the RCP8.5/LTF case. On the other hand, significant runoff decreases during the dry period (from May to September), which also coincide with the irrigation period and, thus, water volumes are diverted before the plants' intake structures, affect the energy generation. For example, in the Axios River, and under the REMO2009/RCP8.5/STF simulation, the averaged discharges from May to September equal  $53.5 \text{ m}^3/\text{s}$  (Figure 5d), while the irrigation water diversions equal  $45.0 \text{ m}^3/\text{s}$ ; hence, the remained low flows are marginal for power production.

#### 4.2. Run-Of-River Small Hydropower Plants and Sustainable Development

Sustainable development, i.e., development without jeopardizing future generations' viability, together with climate change mitigation and adaptation policies, set renewable energy sources as the cornerstones to this effort. Hydropower, as well as all renewables, by default contributes to the reduction of greenhouse gas (GHG) emissions; it is, thus, considered a climate change mitigation asset. In comparison to conventional coal power plants, hydropower prevents the emission of about three GT of  $\text{CO}_2$  per year, or about 9% of global annual  $\text{CO}_2$  emissions [74], with clearness on the debate of hydropower GHG emissions to be given in the literature [75]. At the same time, HPPs, particularly those with reservoirs, are important tools for climate change adaptation; they not only produce clean energy, but they also act as buffers in extreme events imposed by climate change, covering the water demands in case of droughts and protecting the downstream areas in case of floods.

However, the coupling of sustainable development and climate change is a challenging equation still to be solved [76]. Hydropower generation, although a well-established renewable that in many countries is used as a pivotal instrument for sustainable development [15], is mainly conducted through large HPPs whose important environmental and social impacts contradict the sustainable development concept. The European Environment Agency reports that precipitation variability could create uncertainty when investing in hydropower, and, particularly, the increased silting of sediment into reser-

voirs caused by increased erosion and sediment displacement as a consequence of climate change can radically reduce the lifespan of the project [77]. ROR SHPPs, on the other hand, are more so considered as hydro-resilience facilities with minimum dependence of hydraulic head variations [78], as well as installations that could produce energy even in low flows. As friendlier projects with fewer impacts on the environment, e.g., non-affectation of the physico-chemical values of the water quality indicators [79], ROR SHPPs have been gaining interest from policymakers and investors during the last few decades [35], with sustainability indicators for ROR hydroplants to be presented in the literature [80].

## 5. Conclusions

Severe induced climate change impacts on rivers' runoff, as specific climatic models and scenarios foreseen for the end of the 21st century, are bound to affect all hydropower types and schemes. However, run-of-river hydropower plants can produce power even in low flow conditions, thus being able to emerge as hydro-resilience solutions for perennial rivers. Moreover, due to their minimal affect on streamflow timing and volume, they have fewer impacts on the water resources as well as on the dependent anthropogenic and natural environments than other types of SHPPs designs. To sum up, the following concluding remarks may be drawn from this paper:

- ROR SHPPs can easily be adopted in existing irrigation dams without burdening the existing environmental and social footprint caused by the existing dam structures, with modern projects to compulsorily integrate structures for fish passage, as denoted in the European Commission's guidance document on the requirements for hydropower in relation to EU nature legislation, and thus partially restoring the river's discontinuity;
- Simulations triggered by climate change projections; although showing a future decreasing trend of the river discharges in the Mediterranean basin, the attributed impacts to power production differs among the climate models particularly at the seasonal level;
- Since ROR hydro plants have no reservoir for water storage, the timing of the runoff perturbations during the year plays an important role in energy generation. At any case, a large-scale river's discharge decrease (>25.0%) causes important reduction on the generated energy (>20.0%), while for a smaller river's discharge decline (up to 15.0%) no correlation pattern between the discharge decline and the energy generation lessening can be exported.
- In both case study areas, the discharges' decrease occurrence during the wet months partially affects the power production. (e.g., the Kalamas River discharges' decrease of 13.4% cause energy reduction of 2.84% under the RACMO22E/RCP8.5/LTF simulation);
- On the contrary, the impacts on power production are getting higher if the discharge lessening coincides with the dry periods of the year, where the river's runoff is low and competitive water uses such as irrigated agriculture need to be satisfied. (e.g., the Axios River discharges decrease of 5.12% causes an energy decline of 15.81% under the REMO2009/RCP8.5/STF simulation).

To conclude, the proposed outputs shed light on two regions where minimum research have been conducted in terms of climate change: water resources and power generation; while the proposed methodology, which demonstrates the impacts of climate change on run-of-river small hydropower plants, is applicable to all EU basins fragmented with small hydro.

**Funding:** This research received no external funding.

**Institutional Review Board Statement:** Not applicable.

**Informed Consent Statement:** Not applicable.

**Data Availability Statement:** E-HYPE's online data repository for (a) simulated historical daily discharges (<https://hypeweb.smhi.se/explore-water/historical-data/europe-time-series/>) (accessed

on 10 May 2021) at EU scale, and (b) simulated discharges under climate change conditions (<https://hypeweb.smhi.se/explore-water/climate-change-data/europe-climate-change/>) (accessed on 15 May 2021) at EU scale.

**Conflicts of Interest:** The author declares no conflict of interest.

### Abbreviations

E-HYPE: Hydrological Predictions for the Environment for Europe (*hydrological model*); EU: European Union; GHG: Greenhouse gas; HEC-ResSim: Hydrologic Engineering Center-Reservoir System Simulation (*hydropower simulation model*); HPP: Hydropower plant; LTF: Long term future; NSE: Nash–Sutcliffe efficiency coefficient; PCC: Pearson correlation coefficient;  $R^2$ : Coefficient of determination; RCM: Regional Climate Model; RCP: Representative Concentration Pathway; RMSE: Root Mean Square Error; ROR: Run-of-river; REF: Reference period; RES: Renewable energy sources; SHPP: Small Hydropower Plant; SHPP-A: Gitani SHPP on Kalamas River; SHPP-B: Eleousa SHPP on Axios River; STF: Short term future; WD: Water District.

### References

- Kumar, A.; Schei, T.; Ahenkorah, A.; Rodriguez, R.C.; Devernay, J.M.; Freitas, M.; Hall, D.; Killingtveit, Å.; Liu, Branche, E.; et al. *Hydropower IPCC Special Report on Renewable Energy Sources and Climate Change Mitigation*; Cambridge University Press: Cambridge, UK; New York, NY, USA, 2011.
- International Energy Outlook 2021. Available online: [https://www.eia.gov/outlooks/ieo/data/pdf/ref/E01gen\\_r.pdf](https://www.eia.gov/outlooks/ieo/data/pdf/ref/E01gen_r.pdf) (accessed on 25 October 2021).
- Balkhair, K.S.; Rahman, K.U. Sustainable and economical small-scale and low-head hydropower generation: A promising alternative potential solution for energy generation at local and regional scale. *Appl. Energy* **2017**, *188*, 378–391. [[CrossRef](#)]
- Eurostat. Electricity Production, Consumption and Market Overview for Year 2019. Available online: [https://ec.europa.eu/eurostat/statistics-explained/index.php?title=Electricity\\_production,\\_consumption\\_and\\_market\\_overview](https://ec.europa.eu/eurostat/statistics-explained/index.php?title=Electricity_production,_consumption_and_market_overview) (accessed on 13 October 2021).
- Hydropower Europe. Available online: <https://hydropower-europe.eu/about-hydropower-europe/hydropower-energy> (accessed on 1 November 2021).
- De Lucena, A.F.P.; Szklo, A.S.; Schaeffer, R.; de Souza, R.R.; Borba, B.S.M.C.; da Costa, I.V.L.; Pereira Júnior, A.O.; da Cunha, S.H.F. The vulnerability of renewable energy to climate change in Brazil. *Energy Policy* **2009**, *37*, 879–889. [[CrossRef](#)]
- Wachsmuth, J.; Blohm, A.; Gößling-Reisemann, S.; Eickemeier, T.; Ruth, M.; Gasper, R.; Stührmann, S. How will renewable power generation be affected by climate change? The case of a Metropolitan Region in Northwest Germany. *Energy* **2013**, *58*, 192–201. [[CrossRef](#)]
- IPCC. Summary for Policymakers. In *Climate Change 2021: The Physical Science Basis. Contribution of Working Group I to the Sixth Assessment Report of the Intergovernmental Panel on Climate Change*; Masson-Delmotte, V., Zhai, P., Pirani, A., Connors, S.L., Péan, C., Berger, S., Caud, N., Chen, Y., Goldfarb, L., Gomis, M.I., et al., Eds.; Cambridge University Press: Cambridge, UK, 2021; in press.
- IPCC. *Climate Change 2014: Synthesis Report. Contribution of Working Groups I, II and III to the Fifth Assessment Report of the Intergovernmental Panel on Climate Change*; Core Writing Team, Pachauri, R.K., Meyer, L.A., Eds.; IPCC: Geneva, Switzerland, 2014; 151p.
- Sridharan, V.; Broad, O.; Shivakumar, A.; Howells, M.; Boehlert, B.; Groves, D.G.; Rogner, H.-H.; Taliotis, C.; Neumann, J.E.; Strzepek, K.M.; et al. Resilience of the Eastern African electricity sector to climate driven changes in hydropower generation. *Nat. Commun.* **2019**, *10*, 302. [[CrossRef](#)] [[PubMed](#)]
- Cherry, J.E.; Knapp, C.; Trainor, S.; Ray, A.J.; Tedesche, M.; Walker, S. Planning for climate change impacts on hydropower in the Far North. *Hydrol. Earth Syst. Sci.* **2017**, *21*, 133–151. [[CrossRef](#)]
- Mayor, B.; Rodríguez-Muñoz, I.; Villarroja, F.; Montero, E.; López-Gunn, E. The Role of Large and Small Scale Hydropower for Energy and Water Security in the Spanish Duero Basin. *Sustainability* **2017**, *9*, 1807. [[CrossRef](#)]
- Cernea, M. *Hydropower Dams and Social Impacts: A Sociological Perspective*; The World Bank: Washington, DC, USA, 1997.
- Skoulikaris, C.; Kasimis, K. Investigation of climate change impacts on hydropower generation: The case of a run-of-river small hydropower plant in western Greece. *IOP Conf. Ser. Earth Environ. Sci.* **2021**, *899*, 012026. [[CrossRef](#)]
- Dursun, B.; Gokcol, C. The role of hydroelectric power and contribution of small hydropower plants for sustainable development in Turkey. *Renew. Energy* **2011**, *36*, 1227–1235. [[CrossRef](#)]
- Liu, D.; Liu, H.; Wang, X.; Kremere, E. (Eds.) *World Small Hydropower Development Report*; United Nations Industrial Development Organization: Vienna, Austria, 2019.
- Anagnostopoulos, J.S.; Papantonis, D.E. Optimal sizing of a run-of-river small hydropower plant. *Energy Convers. Manag.* **2007**, *48*, 2663–2670. [[CrossRef](#)]

18. Premalatha, M.; Abbasi, T.; Abbasi, S.A. A critical view on the eco-friendliness of small hydroelectric installations. *Sci. Total Environ.* **2014**, *481*, 638–643. [[CrossRef](#)]
19. Skoulikaris, C.; Krestenitis, Y. Cloud Data Scraping for the Assessment of Outflows from Dammed Rivers in the EU. A Case Study in South Eastern Europe. *Sustainability* **2020**, *12*, 7926. [[CrossRef](#)]
20. Hounnou, A.H.; Dubas, F.; Fifatin, F.X.; Chamagne, D.; Vianou, A. Multi-objective optimization of run-of-river small-hydropower plants considering both investment cost and annual energy generation. *World Acad. Sci. Eng. Technol. Int. J. Energy Power Eng.* **2019**, *13*, 17–21.
21. Tamm, O.; Tamm, T. Verification of a robust method for sizing and siting the small hydropower run-of-river plant potential by using GIS. *Renew. Energy* **2020**, *155*, 153–159. [[CrossRef](#)]
22. Kuriqi, A.; Pinheiro, A.N.; Sordo-Ward, A.; Garrote, L. Flow regime aspects in determining environmental flows and maximising energy production at run-of-river hydropower plants. *Appl. Energy* **2019**, *256*, 113980. [[CrossRef](#)]
23. Yildiz, V.; Vrugt, J.A. A toolbox for the optimal design of run-of-river hydropower plants. *Environ. Model. Softw.* **2019**, *111*, 134–152. [[CrossRef](#)]
24. Sachdev, H.S.; Akella, A.K.; Kumar, N. Analysis and evaluation of small hydropower plants: A bibliographical survey. *Renew. Sustain. Energy Rev.* **2015**, *51*, 1013–1022. [[CrossRef](#)]
25. Paish, O. Small hydro power: Technology and current status. *Renew. Sustain. Energy Rev.* **2002**, *6*, 537–556. [[CrossRef](#)]
26. Aggidis, G.A.; Luchinskaya, E.; Rothschild, R.; Howard, D.C. The costs of small-scale hydro power production: Impact on the development of existing potential. *Renew. Energy* **2010**, *35*, 2632–2638. [[CrossRef](#)]
27. Skoulikaris, C.; Ganoulis, J. Multipurpose hydropower projects economic assessment under climate change conditions. *Fresenius Environ. Bull.* **2017**, *26*, 5599–5607.
28. Adynkiewicz-Piragas, M.; Miszuk, B. Risk Analysis Related to Impact of Climate Change on Water Resources and Hydropower Production in the Lusatian Neisse River Basin. *Sustainability* **2020**, *12*, 5060. [[CrossRef](#)]
29. De Souza Dias, V.; Pereira da Luz, M.; Medero, G.M.; Tarley Ferreira Nascimento, D. An Overview of Hydropower Reservoirs in Brazil: Current Situation, Future Perspectives and Impacts of Climate Change. *Water* **2018**, *10*, 592. [[CrossRef](#)]
30. Ehrbar, D.; Schmocker, L.; Vetsch, D.F.; Boes, R.M. Hydropower Potential in the Periglacial Environment of Switzerland under Climate Change. *Sustainability* **2018**, *10*, 2794. [[CrossRef](#)]
31. Maran, S.; Volonterio, M.; Gaudard, L. Climate change impacts on hydropower in an alpine catchment. *Environ. Sci. Policy* **2014**, *43*, 15–25. [[CrossRef](#)]
32. Qin, P.; Xu, H.; Liu, M.; Du, L.; Xiao, C.; Liu, L.; Tarroja, B. Climate change impacts on Three Gorges Reservoir impoundment and hydropower generation. *J. Hydrol.* **2020**, *580*, 123922. [[CrossRef](#)]
33. Savelsberg, J.; Schillinger, M.; Schlecht, I.; Weigt, H. The Impact of Climate Change on Swiss Hydropower. *Sustainability* **2018**, *10*, 2541. [[CrossRef](#)]
34. Totschnig, G.; Hirner, R.; Müller, A.; Kranzl, L.; Hummel, M.; Nachtnebel, H.P.; Stanzel, P.; Schicker, I.; Formayer, H. Climate change impact and resilience in the electricity sector: The example of Austria and Germany. *Energy Policy* **2017**, *103*, 238–248. [[CrossRef](#)]
35. Kelly-Richards, S.; Silber-Coats, N.; Crootof, A.; Tecklin, D.; Bauer, C. Governing the transition to renewable energy: A review of impacts and policy issues in the small hydropower boom. *Energy Policy* **2017**, *101*, 251–264. [[CrossRef](#)]
36. Efthimiou, N. Hydrological simulation using the SWAT model: The case of Kalamas River catchment. *J. Appl. Water Eng. Res.* **2018**, *6*, 210–227. [[CrossRef](#)]
37. Koutsoyiannis, D.; Mamassis, N.; Efstratiadis, A.; Zarkadoulas, N.; Markonis, Y. Floods in Greece. In *Changes of Flood Risk in Europe*; Kundzewicz, Z.W., Ed.; IAHS Press: Wallingford, UK, 2012; pp. 238–256.
38. Skoulikaris, C.; Zafirakou, A. River Basin Management Plans as a tool for sustainable transboundary river basins' management. *Environ. Sci. Pollut. Res.* **2019**, *26*, 14835–14848. [[CrossRef](#)] [[PubMed](#)]
39. Special Secretariat for Water (SSW). *The River Basin Management Plan of Epirus Water District (GR05)*; Ministry of Environment and Energy: Athens, Greece, 2013. (In Greek)
40. Special Secretariat for Water (SSW). *The River Basin Management Plan of Central Macedonia Water District (GR10)*; Ministry of Environment and Energy: Athens, Greece, 2013. (In Greek)
41. Krestenitis, Y.N.; Kombiadou, K.; Androulidakis, Y.S.; Makris, C.; Baltikas, V.; Skoulikaris, C.; Kontos, Y.; Kalantzi, G. Operational Oceanographic Platform in Thermaikos Gulf (Greece): Forecasting and Emergency Alert System for Public Use. In Proceedings of the 36th IAHR World Congress, The Hague, The Netherlands, 28 June–3 July 2015; pp. 5388–5399.
42. US Army Corps of Engineers (USACE). *HEC-ResSim Reservoir System Simulation User's Manual*; Project Report PR-100; Klipsch, J.D., Hurst, M.B., Eds.; US Army Corps of Engineers Institute for Water Resources Hydrologic Engineering Center (HEC): Davis, CA, USA, 2013; p. 556.
43. Kim, J.; Read, L.; Johnson, L.E.; Gochis, D.; Cifelli, R.; Han, H. An experiment on reservoir representation schemes to improve hydrologic prediction: Coupling the national water model with the HEC-ResSim. *Hydrol. Sci. J.* **2020**, *65*, 1652–1666. [[CrossRef](#)]
44. Ozkaya, A.; Zerberg, Y. Water storage change assessment in the Seyhan Reservoir (Turkey) using HEC-ResSim model. *Arab. J. Geosci.* **2021**, *14*, 504. [[CrossRef](#)]
45. Beheshti, M.; Heidari, A.; Saghafian, B. Susceptibility of Hydropower Generation to Climate Change: Karun III Dam Case Study. *Water* **2019**, *11*, 1025. [[CrossRef](#)]

46. Calvo Gobetti, L.E. Application of HEC-ResSim® in the study of new water sources in the Panama Canal. *J. Appl. Water Eng. Res.* **2018**, *6*, 236–250. [CrossRef]
47. Şensoy, A.; Uysal, G.; Şorman, A.A. Developing a decision support framework for real-time flood management using integrated models. *J. Flood Risk Manag.* **2018**, *11*, S866–S883. [CrossRef]
48. Trinh, T.; Jang, S.; Ishida, K.; Ohara, N.; Chen, Z.Q.; Anderson, M.L.; Darama, Y.; Chen, J.; Kavvas, M.L. Reconstruction of Historical Inflows into and Water Supply from Shasta Dam by Coupling Physically Based Hydroclimate Model with Reservoir Operation Model. *J. Hydrol. Eng.* **2016**, *21*, 04016029. [CrossRef]
49. Park, J.Y.; Kim, S.J. Potential impacts of climate change on the reliability of water and hydropower supply from a multipurpose dam in South Korea. *J. Am. Water Resour. Assoc.* **2014**, *50*, 1273–1288. [CrossRef]
50. Shrestha, S.; Khatiwada, M.; Babel, M.S.; Parajuli, K. Impact of climate change on river flow and hydropower production in Kulekhani hydropower project of Nepal. *Environ. Process.* **2014**, *1*, 231–250. [CrossRef]
51. Lindström, G.; Pers, C.; Rosberg, J.; Strömqvist, J.; Arheimer, B. Development and testing of the HYPE (Hydrological Predictions for the Environment) water quality model for different spatial scales. *Hydrol. Res.* **2010**, *41*, 295–319. [CrossRef]
52. Donnelly, C.; Andersson, J.C.; Arheimer, B. Using flow signatures and catchment similarities to evaluate the E-HYPE multi-basin model across Europe. *Hydrol. Sci. J.* **2016**, *61*, 255–273. [CrossRef]
53. Bartosova, A.; Arheimer, B.; De Lavenne, A.; Capell, R.; Strömqvist, J. Large-Scale Hydrological and Sediment Modeling in Nested Domains under Current and Changing Climate. *J. Hydrol. Eng.* **2021**, *26*, 05021009. [CrossRef]
54. Yıldırım, Ü.; Güler, C.; Önel, B.; Rode, M.; Jomaa, S. Modelling of the Discharge Response to Climate Change under RCP8.5 Scenario in the Alata River Basin (Mersin, SE Turkey). *Water* **2021**, *13*, 483. [CrossRef]
55. Arheimer, B.; Donnelly, C.; Lindström, G. Regulation of snow-fed rivers affects flow regimes more than climate change. *Nat. Commun.* **2017**, *8*. [CrossRef] [PubMed]
56. Hundecha, Y.; Arheimer, B.; Donnelly, C.; Pechlivanidis, I. A regional parameter estimation scheme for a pan-European multi-basin model. *J. Hydrol. Reg. Stud.* **2016**, *6*, 90–111. [CrossRef]
57. Pechlivanidis, I.G.; Arheimer, B. Large-scale hydrological modelling by using modified PUB recommendations: The India-HYPE case. *Hydrol. Earth Syst. Sci.* **2015**, *19*, 4559–4579. [CrossRef]
58. Jacob, D.; Petersen, J.; Eggert, B.; Alias, A.; Christensen, O.B.; Bouwer, L.M.; Braun, A.; Colette, A.; Déqué, M.; Georgievski, G.; et al. EURO-CORDEX: New high-resolution climate change projections for European impact research. *Reg. Environ. Chang.* **2014**, *14*, 563–578. [CrossRef]
59. Moss, R.; Edmonds, J.; Hibbard, K.; Manning, M.R.; Rose, S.K.; van Vuuren, D.P.; Carter, T.R.; Emori, S.; Kainuma, M.; Kram, T.; et al. The next generation of scenarios for climate change research and assessment. *Nature* **2010**, *463*, 747–756. [CrossRef] [PubMed]
60. Teichmann, C.; Eggert, B.; Elizalde, A.; Haensler, A.; Jacob, D.; Kumar, P.; Moseley, C.; Pfeifer, S.; Rechid, D.; Remedio, A.R.; et al. How does a regional climate model modify the projected climate change signal of the driving GCM: A study over different CORDEX regions using REMO. *Atmosphere* **2013**, *4*, 214–236. [CrossRef]
61. Van Meijgaard, E.; van Ulft, L.H.; van de Berg, W.J.; Bosveld, F.C.; van den Hurk, B.; Lenderink, G.; Siebesma, A.P. *The KNMI Regional Atmospheric Climate Model RACMO Version 2.1*; Technical Report, TR 302; KNMI: De Bilt, The Netherlands, 2008.
62. Strandberg, G.; Bärring, L.; Hansson, U.; Jansson, C.; Jones, C.; Kjellström, E.; Kupiainen, M.; Nikulin, G.; Samuelsson, P.; Ullerstig, A. CORDEX scenarios for Europe from the Rossby Centre regional climate model RCA4. In *Reports Meteorology and Climatology; SMHI: Norrköping, Sweden, 2015*; Volume 116, SE-601 76.
63. Kuentz, A.; Arheimer, B.; Hundecha, Y.; Wagener, T. Understanding hydrologic variability across Europe through catchment classification. *Hydrol. Earth Syst. Sci.* **2017**, *21*, 2863–2879. [CrossRef]
64. Kapetas, L.; Kazakis, N.; Voudouris, K.S.; Martinez-Tello, A.; Hosking, S. Modelling groundwater-surface water interactions under climate change scenarios: Insights from Axios Delta, Greece. In *Proceedings of the 2nd International Conference on Natural Hazards and Infrastructure 2019, Chania, Greece, 23–26 June 2019*.
65. Poulos, S.E.; Ghionis, G.; Maroukian, H. The consequences of a future eustatic sea-level rise on the deltaic coasts of Inner Thermaikos Gulf (Aegean Sea) and Kyparissiakos Gulf (Ionian Sea), Greece. *Geomorphology* **2009**, *107*, 18–24. [CrossRef]
66. Monevska, S.A. Climate Changes in Republic of Macedonia. In *Climate Change and Its Effects on Water Resources*; NATO Science for Peace and Security Series C: Environmental, Security; Baba, A., Tayfur, G., Gündüz, O., Howard, K., Friedel, M., Chambel, A., Eds.; Springer: Dordrecht, The Netherlands, 2011; Volume 3. [CrossRef]
67. Granados, A.; Sordo-Ward, A.; Paredes-Beltrán, B.; Garrote, L. Exploring the Role of Reservoir Storage in Enhancing Resilience to Climate Change in Southern Europe. *Water* **2021**, *13*, 85. [CrossRef]
68. PeSPKA Hpeiros (Regional Plan of the Region of Epirus on Climate Change Adaption). Available online: <http://emvis.gr/index.php/peSPKA> (accessed on 14 October 2021).
69. Papadaki, C.; Dimitriou, E. River Flow Alterations Caused by Intense Anthropogenic Uses and Future Climate Variability Implications in the Balkans. *Hydrology* **2021**, *8*, 7. [CrossRef]
70. Vrzel, J.; Ludwig, R.; Gampe, D.; Ogrinc, N. Hydrological system behaviour of an alluvial aquifer under climate change. *Sci. Total Environ.* **2019**, *649*, 1179–1188. [CrossRef]

71. Herrero, A.; Gutiérrez-Cánovas, C.; Vigiak, O.; Lutz, S.; Kumar, R.; Gampe, D.; Huber-García, V.; Ludwig, R.; Batalla, R.; Sabater, S. Multiple stressor effects on biological quality elements in the Ebro River: Present diagnosis and predicted responses. *Sci. Total Environ.* **2018**, *630*, 1608–1618. [[CrossRef](#)]
72. Gaudard, L.; Avanzi, F.; De Michele, C. Seasonal aspects of the energy-water nexus: The case of a run-of-the-river hydropower plant. *Appl. Energy* **2018**, *210*, 604–612. [[CrossRef](#)]
73. Ludwig, W.; Dumont, E.; Meybeck, M.; Heussner, S. River discharges of water and nutrients to the Mediterranean and Black Sea: Major drivers for ecosystem changes during past and future decades? *Prog. Oceanogr.* **2009**, *80*, 199–217. [[CrossRef](#)]
74. Berga, L. The role of hydropower in climate change mitigation and adaptation: A review. *Engineering* **2016**, *2*, 313–318. [[CrossRef](#)]
75. Liden, R. *Greenhouse Gases from Reservoirs Caused by Biochemical Processes: Interim Technical Note*; World Bank: Washington, DC, USA, 2013.
76. Bildirici, M.E.; Gökmenoğlu, S.M. Environmental pollution, hydropower energy consumption and economic growth: Evidence from G7 countries. *Renew. Sustain. Energy Rev.* **2017**, *75*, 68–85. [[CrossRef](#)]
77. EEA. *Climate Change, Impacts and Vulnerability in Europe 2016-An Indicator-Based Report*; Report No 1/2017; European Environment Agency: Copenhagen, Denmark, 2017.
78. Phillips, T.; Chalishazar, V.; McJunkin, T.; Maharjan, M.; Alam, S.S.; Mosier, T.; Somani, A. A metric framework for evaluating the resilience contribution of hydropower to the grid. In Proceedings of the 2020 Resilience Week (RWS), Salt Lake City, ID, USA, 19–23 October 2020; pp. 78–85.
79. Česonienė, L.; Dapkienė, M.; Punys, P. Assessment of the Impact of Small Hydropower Plants on the Ecological Status Indicators of Water Bodies: A Case Study in Lithuania. *Water* **2021**, *13*, 433. [[CrossRef](#)]
80. Kumar, D.; Katoch, S.S. Sustainability indicators for run of the river (RoR) hydropower projects in hydro rich regions of India. *Renew. Sustain. Energy Rev.* **2014**, *35*, 101–108. [[CrossRef](#)]